Alpha B-crystallin in corpora lutea of pseudopregnant rat

Raivo Masso, Anu Saag, Andres Arend[1], Marika Masso, Gunnar Selstam[2]
Department of General and Molecular Pathology, [1]Department of Anatomy, University of Tartu, Estonia, [2]Department of Cell and Molecular Biology, University of Umeå, Sweden

Keywords: *small heat shock protein, alpha B-crystallin, corpus luteum, immunohistochemistry, cytoskeleton.*

Summary. *Localization sites and labeling intensity of αB-crystallin in corpus luteum (CL) of pseudopregnant rats has been studied using postembedding light and electron microscopical immunohistochemistry. At days 2 and 18 αB-crystallin labeling was found to be significantly higher compared with the luteal maintenance period (days 6 and 10). αB-crystallin localized both to luteal and interstitial cells of CL.*

At light microscopical level αB-crystallin labeling decreased during CL life span in the central area of luteal cells cytoplasm and increased in the peri-plasmalemmal area. Interstitial cells labeling was found to increase at day 6, followed by almost complete disappearance during functional luteolysis (days 15 and 18).

Our results at electron microscopical level showed αB-crystallin to localize in cytoplasm with close relationship with endoplasmic reticulum, Golgi apparatus, mitochondria and also in nuclei of luteal and interstitial cells. At day 2 labeling of luteal cells was abundant in cytoplasm but weak in nuclei. During the luteal maintenance period and functional luteolysis labeling in luteal cells was relocalized to the peri-plasmalemmal and perinuclear areas. Labeling in nuclei of luteal cells was weak. At the same time (day 6) interstitial cells including nuclei showed strong labeling, which was significantly decreased during luteolysis.

Immunohistochemically detectable tubulin decreased in CL tissue during CL life span allowing to suggest that αB-crystallin acts as chaperone, one possible role of which is to stabilize the cytoskeleton in different CL cell types during CL formation and active functioning.

Introduction

Alpha B-crystallin is known as a cytosolic, small heat shock-like multimeric protein (molecular weight 20 kDa for subunits) that has anti-aggregation, chaperone-like properties (for review see 1, 2). The expression of the αB-crystallin gene is developmentally regulated and induced by a variety of stress stimuli. Although originally thought of as only contributing to the structural and refractive properties of the lens, αB-crystallin is not restricted to the lens and may have wider functional significance. The extra-lenticular expression of αB-crystallin has been reported in many tissues (2). Alpha B-crystallin co-localizes with intermediate filaments during stress, which includes vimentin (3) and keratin intermediate filaments (4), and also with β-tubulin (5). This association of αB-crystallin with cytoskeletal elements during heat shock or stress could indicate that the chaperone function of αB-crystallin protects cellular integrity.

According to our knowledge, there are no investigations concerning the detection of αB-crystallin in corpus luteum (CL) tissue and in different cell types of CL during pregnancy or/and pseudopregnancy. The present study was undertaken to detect αB-crystallin localization in CL of pseudopregnant rats at tissue and subcellular levels and to find a correlation between αB-crystallin and cellular cytoskeletal elements during CL life span.

Materials and methods

Animals. Adult female Sprague-Dawley rats were used. The rats were housed in controlled environmental conditions (22° C, 45–55% humidity, lights on between 06.00 to 18.00 hs) and had free access to standard pellets and tap water. All experimental protocols were approved by the Animal Experimentation Ethical Committee of Umeå University, Sweden.

To induce pseudopregnancy, female rats were mated with sterile male rats. Animals were sacrificed by decapitation at 13.00 h at day 2, 6, 10, 13, 15 and 18 of

Correspondence to R. Masso, Department of General and Molecular Pathology, University of Tartu, Ravila 19, 50411 Tartu, Estonia. E-mail: masso@ut.ee

pseudopregnancy (n=5 at each time-point).

Sampling. The ovaries were quickly extirpated and tissue was fixed with solution, which consists of 0.5% paraformaldehyde, 2.5% glutaraldehyde and 0.1% picric acid, all in 0.1 M phosphate buffer (pH 7.4) for 2 hours at a room temperature. Individual CLs were separated and fixed additionally in 2.5% glutaraldehyde in 0,1 M phosphate buffer, pH 7.4, 1 h at a room temperature, then washed in buffer containing 1% of bovine serum albumin fraction V (Sigma Chemicals, St. Louis, MO, USA), incubated for 1 h with 50 mM NH_4 OH in buffer to eliminate glutaraldehyde, dehydrated in a series of graded alcohol, stained en bloc with 1% uranyl acetate solution in 70° ethanol for 1 h and embedded into Epon-812 mixture. Blocks were polymerized for 24 hours at 50° C.

Antibodies. Following primary antibodies were used: Polyclonal rabbit antibody against human alpha B-crystallin residues 1–10 (Novocastra Laboratories, Newcastle-upon-Tyne, UK); Monoclonal anti-tubulin antibody (Ab-4, clone DM1A+DM1B, NeoMarkers, USA); Monoclonal anti-vimentin antibody (clone V9, mouse IgG1 isotype, Sigma. Secondary antibodies used were Goat anti-rabbit IgG labeled with 20 nm colloidal gold particles or Goat anti-mouse antibody labeled with 20 nm colloidal gold particles (Pelco International, Redding, CA, USA).

To demonstrate specificity of the immunogold labeling the primary antibody was omitted in control sections (both for immunohistochemistry and immunocytochemistry) – sections were incubated with the antibody diluent only, followed by the nanogold probe.

Immunohistochemistry. Light microscopical immunohistochemistry was performed on semithin sections (1 mm) cut on the LKB V (LKB-Produkter AB, Sweden) ultramicrotome and collected on BioBond tissue section adhesive (British BioCell International) coated microscope slides, counterstained after performing immunoreactions with methylene blue and mounted into BioMount tissue mounting medium (British BioCell International). For immunohistochemical investigation 3–5 different CLs (from different rats) at each time-point (days 2, 6, 10, 15 and 18) were used. Blocks were trimmed in a way that all different regions of CL were included (theca, granulosa or luteal cells and central interstitial region). A set of serially cut semithin sections was made of each CL (22 slices, every 3rd slice was collected, all together 8 semithin sections from each CL). The starting site for sectioning was randomly selected near the "equatorial" layer of CL.

Immunoreactions for light microscopical immunohistochemistry combined following steps:

1) blocking of non-specific binding with solution consisting of 1% (v/v) of cold-water fish skin gelatin (Sigma) and 1% (v/v) of heat-inactivated normal goat serum in Tris buffered saline (TBS, 0.05 M Tris, 0.15 M NaCl, 0.0025 M KCl, pH=7.6) in a humid chamber at +4°C for 12 h or for 1 hour at a room temperature; 2) washing in TBS (5 changes, 5 min. each); 3) incubating with primary antibody in 1:100 or 1:200 dilution in TBS for 1 hour at a room temperature in a humid chamber or overnight (16–18 hours) in a humid chamber at +4°C; 4) rinsing with TBS with 0.1% Tween-20 (Sigma), three times for 10 minutes; 5) incubating with secondary antibody labeled with 20 nm colloidal gold particles in 1:100 dilution in TBS for 1 hour at a room temperature in a humid chamber. To avoid non-specific binding with aggregated nanogold complexes the solution was previously centrifuged for 10 min. at 1250 g; 6) rinsing with TBS with 0.1% Tween-20 (3×10 min.) and bidistilled deionized water (3×10 min) followed by air-drying; 7) processing with BioCell LM/EM Silver Enhancing Kit (British BioCell International) to make a nanogold label visible at light microscope level (5–10 min., final diameter of dots 200 nm); 8) careful washing with deionized bidistilled water and air-drying. Sections were counterstained with toluidine blue and mounted with BioMount.

Immunocytochemistry. For immunocytochemical investigations 3–5 different CLs (from different rats) at each time-point (day 2, day 6, day 11, day 13 and day 18) were used. Thin (60 nm) sections were cut from Epon-812 blocks on an RMC MT-XL ultramicrotome (Boeckeler Instruments, Inc., Tuscon, AZ, USA) and collected on 150 mesh nickel grids (Sigma). Immunoreactions for immunocytochemistry combined following steps: 1) blocking non-specific binding on a 25 ml droplet of a blocking solution for 30 min. at a room temperature, a section face down. The blocking solution consisted of 0.1% Tween-20, 1% (v/v) cold-water fish skin gelatin (Sigma) and 5% (v/v) heat-inactivated normal goat serum, all in Tris buffered saline (TBS, 0.05 M Tris, 0.14 M NaCl, 0.0027 M KCl, pH=7.6); 2) incubating on the surface of a 25 ml droplet with primary antibody in 1:100 or 1:200 dilution in TBS for 1 hour at a room temperature or overnight (16–18 hours) in a humid chamber at +4°C; 3) rinsing with TBS with 0.1% Tween-20, three times for 10 minutes; 4) incubating on the surface of a 25 ml droplet with secondary antibody labeled with 20 nm colloidal gold particles in 1:100 dilution in TBS. To avoid non-specific binding with aggregated nanogold complexes the solution was previously centrifuged for 10 min at 1250 g; 5) rinsing with TBS with 0.1% Tween-20 (3×10 min.) and bidistilled deionized water (3×10 min.); 6) stabilization of immunocomplexes with

2% water solution of glutaraldehyde, 5 min at room temperature; 7) careful washing with bidistilled deionized water to remove unbound gold conjugate: dipping of grids into water, 60 strokes, 2 changes, and 3×10 min. on a droplet of water and air-drying; 8) staining of sections with 2% osmium tetroxide, uranyl acetate and lead citrate. The grids were examined and photographed using Philips Tecnai 10 or JOEL 1200 EX II transmission electron microscopes.

Image analysis. Quantitative and qualitative methods of image analysis were both used. For qualitative evaluation of immunolabel localization at light microscope and electron microscope levels in different cells (luteal cells, interstitial cells) and different cellular compartments of luteal cells a semiquantitative scale was used. Computer-assisted quantitative image analysis was based on the technical set-up including an Olympus BX 50 microscope (Olympus Optical; Tokyo, Japan) and a digital camera (Camedia C-2020Zoom, Olympus Optical, Japan). At least 10 microscopic fields were captured for analyses from each semithin section at the final magnification 1833x. The software used for counting of silver dots was Adobe Photoshop, version 5.0 (Adobe Systems; Mountain View, CA, USA). Using the Magic Wand tool in the Select menu of Adobe Photoshop the dark black area of silver label was selected. The Similar command in the Select menu allowed all immunolabels to be selected automatically. An optical density plot was generated using the Histogram tool in the Image menu (6). The value of labeled pixels was recorded in the Microsoft Excel worksheet.

Statistical analysis. Unpaired tests were performed between the groups with Student's two-tailed t-test using the Microsoft Excel statistical package. All values are means ±SE. Statistical significance was defined as $p<0.05$.

Results

Localization and intensity of alpha B-crystallin labeling in corpus luteum of rat. In the study we evaluated the labeling intensity and the cellular distribution of αB-crystallin in CL of pseudopregnant rats using postembedding light microscopical immunohistochemical method with antibodies against αB-crystallin and nanogold-labeled secondary antibodies. We found the total labeling in CL tissues for αB-crystallin to be significantly higher at day 2 and day 18, compared with the luteal maintenance period (days 6 and 10). Immunohistochemically detectable αB-crystallin content in the whole CL tissue decreased significantly during pseudopregnancy and had minimum level at days 6 and 10, in the luteal maintenance period, and also at day 15, when the luteal regression period began (Fig. 1).

During the CL life span we found also changes in the localization of immunolabels at light microscope level in luteal and interstitial cells (Table and Fig. 2).

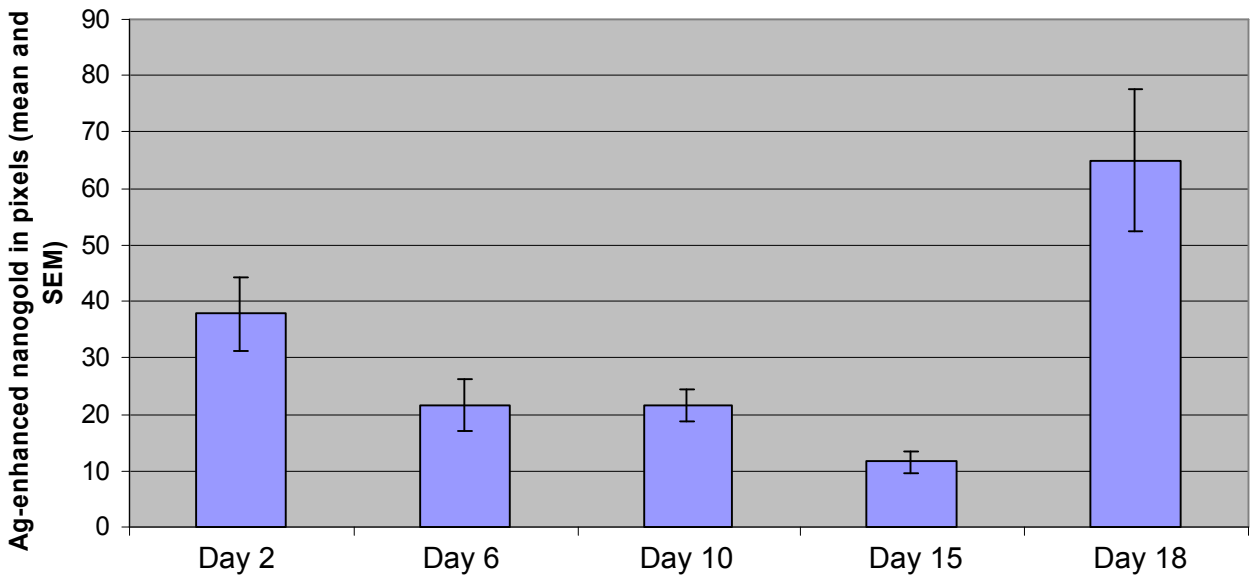

Differences are significant at $p<0.05$: day 2 vs day 15, day 2 vs day 10, day 18 vs day 15, day 18 vs day 10 and day 18 vs day 6.

Fig. 1. **Changes in the amount of αB-crystallin immunolabeling during pseudopregnancy in rat corpora lutea**
Silver-enhanced nanogold label of secondary antibody, in pixels, mean ± SEM.

At day 2, in the period of luteal development, abundant immunolabeling was found in luteal cells, where it mostly located in the central region of cytoplasm and in perinuclear area. Labels were found also in nuclei of luteal cells. At the same time interstitial cells (endothelial cells, pericytes, macrophages) showed a weak labeling and their nuclei were almost devoid of labels. During the luteal maintenance period (days 6 and 10) labeling was seen in luteal and interstitial cells. In interstitial cells and especially inside their nuclei the de-

Table. **Evaluation of αB-crystallin localization in corpora lutea of pseudopregnant rat**

Time point	Luteal cells				Interstitial cells
	central cytoplasm	peri-plasmalemmal cytoplasm	perinuclear cytoplasm	nucleus	
Day 2	+++	+	++	+	+
Day 6	++	+++	++	+	++++
Day 10	+	+	+	+	++
Day 15	0	++	+	+	+
Day 18	0	+++	+	+	0

Semiquantitative scale of evaluation: 0 – labeling is very weak, + – labeling is weak, ++ – labeling is moderate; +++ – labeling is strong; ++++ – labeling is very strong.

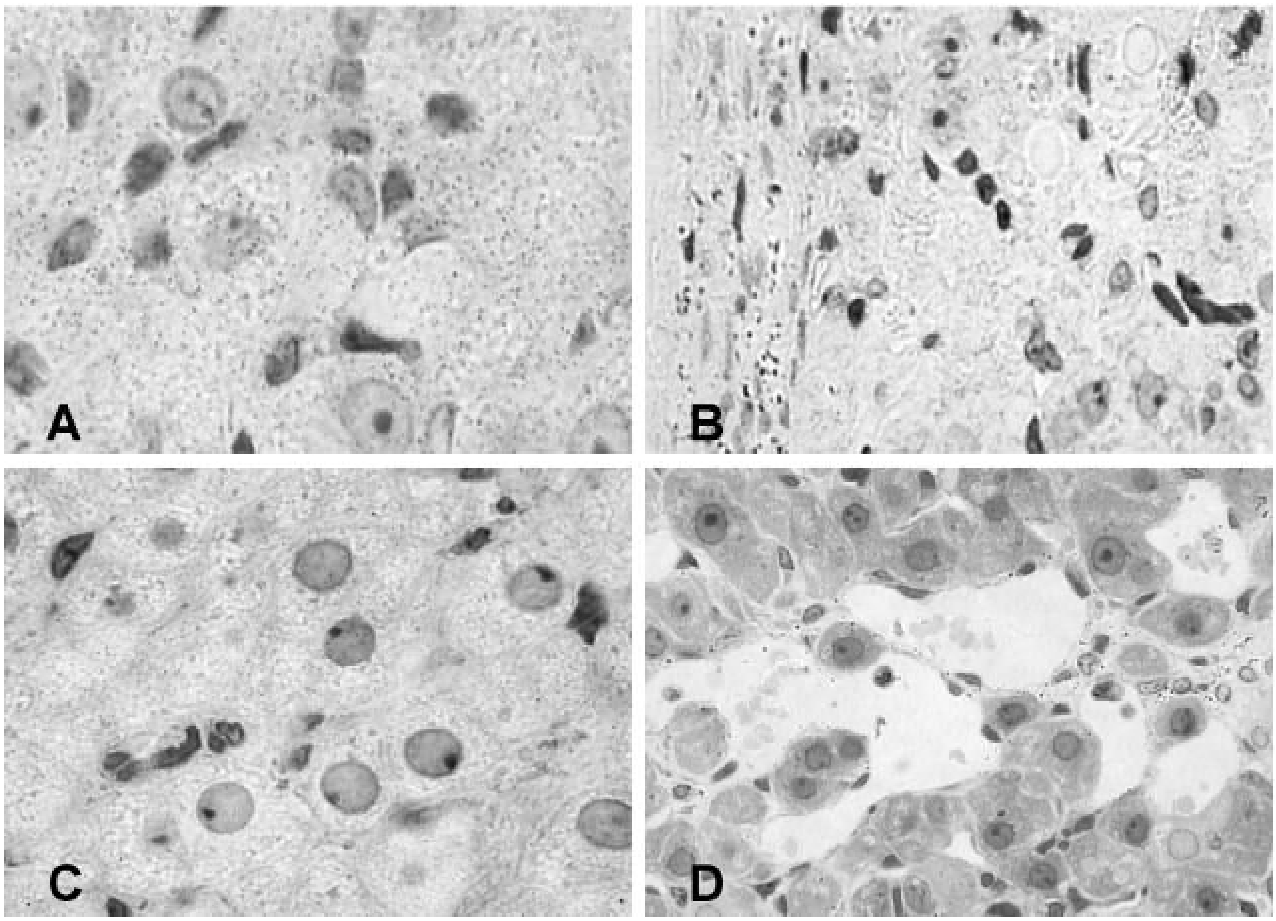

Fig. 2. **Immunohistochemical localization of αB-crystallin (A, B, C) and tubulin (D) in corpus luteum tissue of pseudopregnant rat. Silver enhanced nanogold label counterstained with toluidine blue, semithin sections**

αB-crystallin labeling is abundant in luteal tissue at day 2 (A), decreases at day 10 in luteal tissue showing still abundant labeling in theca layer (B) and is weak in luteal tissue at day 15 (C). Tubulin labeling locates in interstitial cells and decreases during CL life span (D, day 15). Magnification: ×1000 (A), ×500 (B), ×900 (C) and ×700 (D).

tectable increase in immunolabel was observed. Inside luteal cells labels were found mostly at peri-plasmalemmal region of cytoplasm, whereas localization of label at perinuclear area was weaker than at day 2. Label was also found inside nuclei of luteal cells. During the luteal regression period or functional luteolysis (days 15 and 18) immunolabeling in luteal cells was found to disappear from the central area of cytoplasm, to diminish in the perinuclear area, in nuclei, and to accumulate in peri-plasmalemmal region. The level of immunohistochemically detectable αB-crystallin in CL tissue was the highest at these days. All the labeling was found to locate in luteal cells as endothelial cells were devoid of immunohistochemically detectable αB-crystallin.

Changes in tubulin and vimentin immunolocalization. According to qualitative evaluation immunohistochemically detectable tubulin (Fig. 2) decreases during CL life span. At day 2 and 6 visible amounts of tubulin were in interstitial cells. From the day 10 immunolabeling decreased and only few labels were found at day 18. Immunohistochemically detectable vimentin labeling was weak and changes in amounts of vimentin during pseudopregnancy were not detected.

Electron microscopical immunocytochemical localization of alpha B-crystallin in CL. Our results on electron microscopical level showed that immunocytochemically detectable αB-crystallin in luteal cells and interstitial cells of the CL tissue locates to cytoplasm with close relationship with endoplasmic reticulum, Golgi apparatus and also in mitochondria, and in nuclei of luteal and interstitial cells. During life span of CL changes in the labeling intensity and localization were found. At the development of CL (day 2) labeling was abundant in cytoplasm of luteal cells but weak in nuclei. Interstitial cells were weakly labeled and their nuclei were devoid of labels (Fig. 3).

During the luteal maintenance period (days 6 and

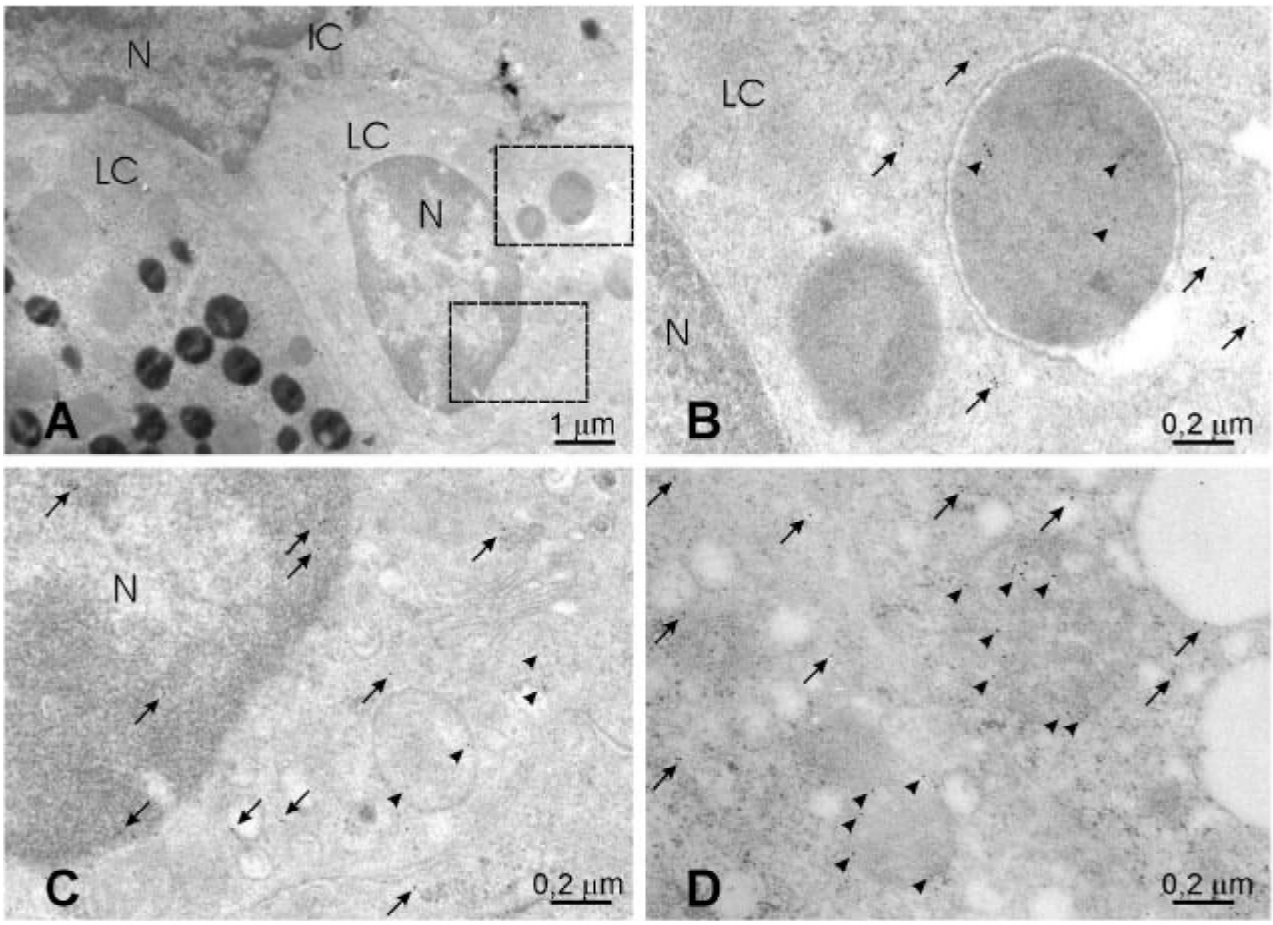

Fig. 3. **Immunocytochemical localization of αB-crystallin in corpus luteum tissue of pseudopregnant rat at luteal development (day 2). Osmium-free fixation**

A – parts of luteal cells (LC) and interstitial cell (IC). Perinuclear areas of luteal cell (in rectangles) are shown separately (B and C) at higher magnification. C – central cytoplasm area of luteal cell at higher magnification. In both perinuclear (B, C) and central cytoplasm areas (D) label locates in cytoplasm with close relationship with endoplasmic reticulum, Golgi apparatus (arrows) and in mitochondria (arrowheads). N – nucleus.

11) amounts of gold particles in luteal cell cytoplasm seemed to decrease slightly but more labeling was found in mitochondria. Labeling in luteal cells was more abundant at the periphery of cytoplasm, the peri-plasmalemmal and the perinuclear areas but weak in nuclei. At the same time, especially at day 6, labeling of interstitial cells was abundant. Gold particles were numerously found in nuclei of endothelial cells, pericytes and macrophages, where it locates by the perimeter of heterochromatin area (Fig. 4).

At day 13 labeling in luteal cells was located again mostly in the perinuclear area, where accumulation of gold particles was found with close connection of cytoskeletal fibers. Strong labeling was detected in nuclei also (Fig. 5). At the time of active luteolysis, day 18 (Fig. 5), no changes compared to day 13 were found in luteal cells. Labeling was found in the peri-plasmalemmal and perinuclear areas and in nuclei of luteal cells. At the same time labeling was weak in cytoplasm and nuclei of endothelial cells. Surprisingly some interstitial cell types, probably macrophages showed abundant labeling, especially in their nuclei.

Discussion

Small heat shock proteins (sHsps) constitute one of the major heat shock protein families and are characterized by the molecular mass of 15–42 kDa. Initially thought to be lens-specific protein, αB-crystallin has been identified also in many other tissues (2). According to our knowledge, αB-crystallin in ovary tissues has not been studied but it is found in clearly detectable amounts in cultured ovarian carcinoma cells (7).

The results of our study demonstrate the ability of both luteal and interstitial cells of the pseudopregnant rat CL to show presence of αB-crystallin. Total immunolabeling for αB-crystallin detected at light microscope level decreased during pseudopregnancy. The

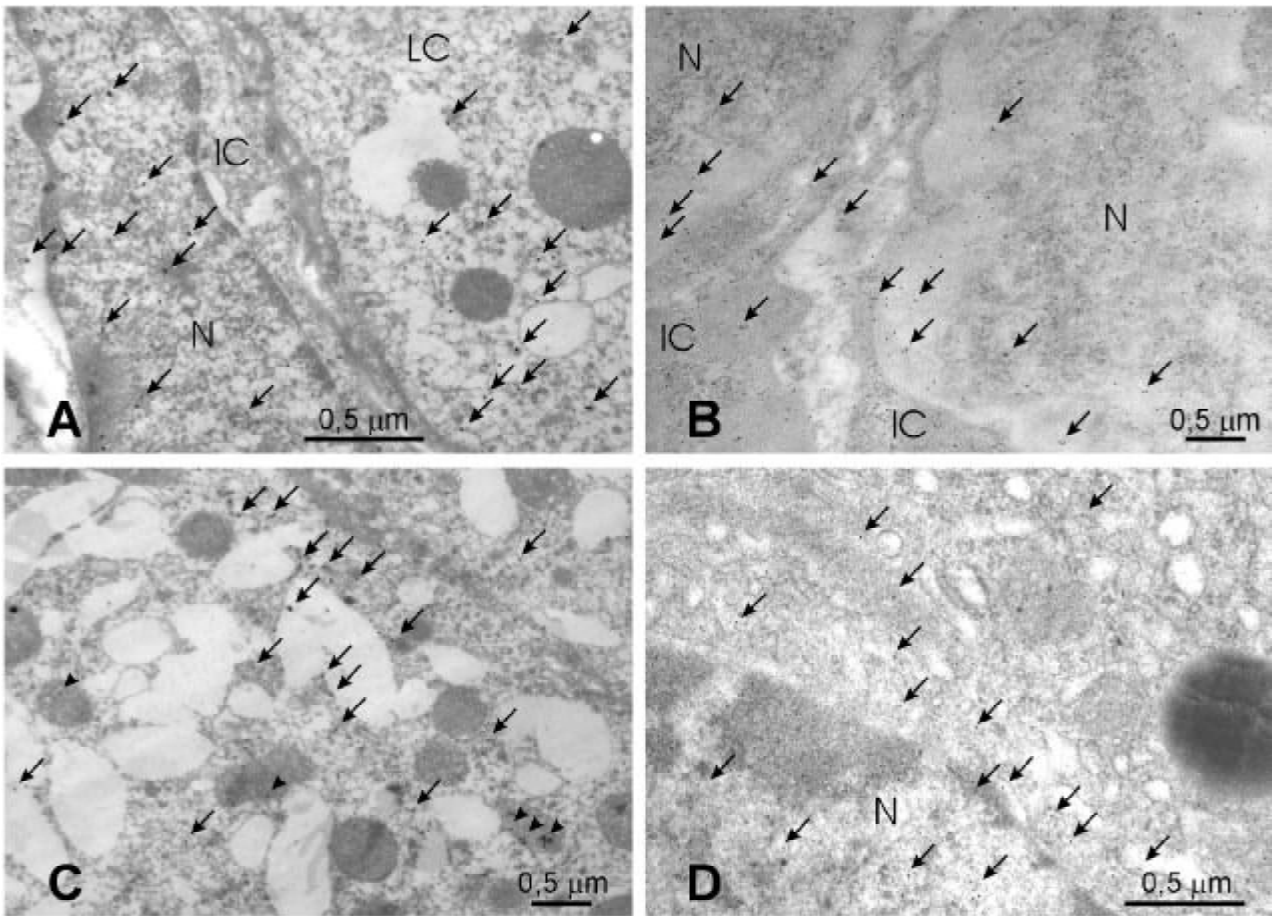

Fig. 4. **Immunocytochemical localization of αB-crystallin in corpus luteum tissue of pseudopregnant rat at day 6. Osmium-free fixation**

Localization of label in nuclei of interstitial cells (A, B), in nuclei of luteal cells (C, D), in peri-plasmalemmal area of luteal cell (A) and perinuclear area of luteal cell (C, D). IC – interstitial cell; LC – luteal cell; N – nucleus; arrows – label in cytoplasm, endoplasmic reticulum or nucleus; arrowhead – label in mitochondria.

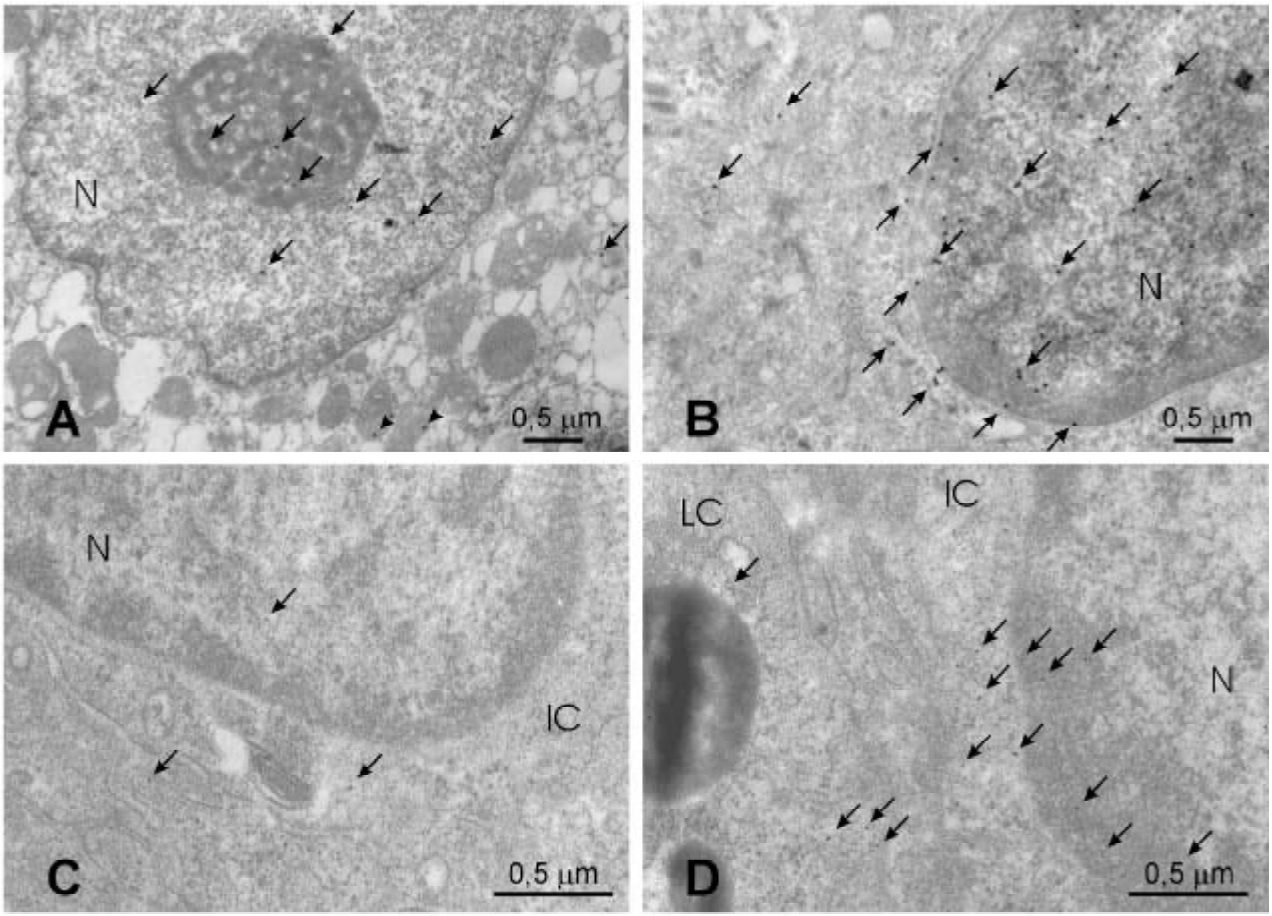

Fig. 5. **Immunocytochemical localization of αB-crystallin in corpus luteum of pseudopregnant rat at days 11 (A), 13 (B) and 18 (C, D). Osmium-free fixation**

Moderate amount of label in luteal cell (A) nucleus and cytoplasm and abundant labeling in interstitial cell nucleus (B) at days 11 and 13. At day 18 interstitial cells were very weakly labeled (C) with exception of few cells (D).

maximal values were at day 2, at the time when CL was developing, and at day 18, at the end of functional luteolysis when structural luteolysis or apoptosis began. We showed that during final stages of CL life span αB-crystallin disappeared from interstitial cells of CL. The biological role of αB-crystallin and other members of sHsp family is believed to act as molecular chaperones and to have cytoprotective activity in a variety of human diseases, including ischemia, inflammation, and infection in vitro and *in vivo* (1, 2). We can suggest that up-regulation of αB-crystallin synthesis in the last stage of CL life span is to maintain cells integrity during luteolysis and when the protective capacity is exhausted, structural luteolysis is initiated. It is supported by our preliminary results demonstrating low levels of αB-crystallin at day 21 (data not shown).

Our results at electron microscopical level showed that immunocytochemically detectable αB-crystallin in luteal cells and interstitial cells of CL tissue was localized in cytoplasm with close relationship with endoplasmic reticulum, Golgi apparatus and also in mitochondria, and in nuclei of luteal and interstitial cells. During life span of CL changes in localization sites could be followed. At day 2 cytoplasm of luteal cells was abundantly and diffusely labeled but at days 6 and 10 labeling attained peripheral location at periplasmalemmal and perinuclear regions. At the later stages the same peripheral localization pattern was seen in cytoplasm with much higher labeling in nucleus. The same phenomenon of labeling relocalization in interstitial cells could be detected. At day 2 labeling was weak in cytoplasm and missing in nucleus, at days 6 and 10 it was equally strong in nucleus and cytoplasm, followed by decrease at days 13 and 18. Surprisingly only macrophages at day 18 showed intensive labeling. This finding of labeling relocalization is in accordance with the study of R. Klemenz, et al (8) showing cytoplasmic αB-crystallin to be translocated upon heat shock to the insoluble fraction, perinuclear and membrane regions. It is also shown that in astro-

cytes exposed to stress αB-crystallin is condensed in granules around the nucleus and co-localized with intermediate filaments (9).

αB-crystallin is known to act as chaperone for actin microfilaments, desmin intermediate filaments (10), and tubulin subunits of microtubules (11) protecting them from heat shock and oxidative stress-induced damage (12). Cytoskeleton plays an important role in a corpus luteum function. After the formation of corpus luteum, both granulosa and theca cells express immunoreactivity for vimentin and in the luteinized granulosa cells immunoreactivity for cytokeratins, desmin (13) and tubulin was detected (14). G. Selstam et al. (15) showed immunohistochemically in pseudopregnant rats that desmin was localized mainly in vascular smooth muscle cells with increase in content after day 6. Results of our study, especially detected changes in αB-crystallin distribution in different CL cell types and parallel changes in tubulin amounts allow us to speculate that relocalization of immunohistochemically detectable αB-crystallin during CL life span may be explained through its action on cytoskeleton components.

According to qualitative evaluation, immunohistochemically detectable tubulin labeling was decreased during CL life span. At day 2 and day 6 of pseudopregnancy visible amounts of tubulin were in interstitial cells. From the day 10, tubulin labeling decreased and only few labels were found in CL tissue at day 18. Visible changes in vimentin immunostaining in CL during pseudopregnancy were not detected. It is in accordance with the study of I. Nilson et al. (16) showing no changes in the immunohistochemical staining intensity of vimentin in a blood vessel of endothelial cells and cytokeratins in theca layer cells in pseudopregnant rat CL. We were able to show only weak immunostaining of vimentin mostly inside cytoplasm of interstitial cells. The association of filaments and microtubules with αB-crystallin is thought to stabilize the cytoskeletal structures (17) as interaction of filament network with αB-crystallin has been visualized by electron microscopy revealing αB-crystallin particles to decorate filaments (3, 18).

In the present study we found translocation of immunolabel from cytoplasm to nuclei and decreased labeling of interstitial cell nuclei at the time of luteolysis. The role of αB-crystallin in nuclei is still unsolved. It has been shown in cultured Chinese hamster ovary cells that during cell division αB-crystallin was excluded from condensed chromatin, however, the protein again appears in newly formed nuclei after the completion of cytokinesis suggesting a conditional, regulatory role for αB-crystallin in cell nucleus (19). W. M. Xiao et al. (20) showed αB-crystallin translocation from cytoplasm to nucleus in cardiomyocytes. Recently was found that sHsp27, very close to αB-crystallin, binds in nucleus to special cell death inhibiting RNA (CDIR), which forms complex with AUF1 (regulator of mRNA turnover) and has anti-apoptotic function (21). These investigators have also speculated that sHsp27 in nuclei might modulate AUF1 activity as it was reported to regulate cyclooxygenase-2 (COX-2) mRNA stability through an AUF1-binding element (22). M. C. Kamradt et al. (23) have shown that αB-crystallin inhibits both the mitochondrial and death receptor apoptotic pathways and that (24) expression of αB-crystallin, but not sHsp27, is sufficient to inhibit differentiation-induced myoblast apoptosis and that αB-crystallin negatively regulates differentiation-induced myoblast apoptosis by inhibiting the proteolytic activation of caspase-3. In our study we have also found an accumulation of αB-crystallin in mitochondria, especially at day 6 when CL functions with maximal activity. During the luteolysis (from day 13), which is characterized by the destruction of cellular structures, labeling in mitochondria was decreased.

There is experimental evidence that αB-crystallin expression is enhanced by prostaglandins (25). Inhibitors of cyclooxygenases and lipoxygenases and activators of phospholipase A_2 stimulate the induction of αB-crystallin *in vitro* during heat or arsenite stress – a response, which was also shown with aspirin *in vivo* in the adrenal glands and other tissues (26). In ewes, induction of luteolysis by treatment with prostaglandin $F_{2\alpha}$ rapidly and dramatically reduces the number of luteal cells staining positive for tubulin (14). The disappearance of tubulin occurs before decreased luteal concentrations of progesterone, indicating that disruption of the cytoskeleton precedes decreased synthesis of progesterone. However, it is not clear whether disruption of the microtubule network prevents transport of cholesterol to mitochondria or disturbs other aspects of luteal steroidogenesis. Thus prostaglandin $F_{2\alpha}$-induced disruption of the cytoskeleton may impair synthesis of progesterone early during luteolysis. During functional luteolysis morphological changes in steroidogenic luteal cells do not become evident until 36 hours after exposure to prostaglandin $F_{2\alpha}$, although the steroidogenic capacity of the cells is markedly reduced by this time (27). At the same time endothelial cells in capillaries of CL from ewes exhibit dramatic morphological changes that are indicative of apoptosis (28). It is suspected that degeneration of endothelial cells is a direct effect of prostaglandin $F_{2\alpha}$ but this has not been proven.

Conclusions

In this study, we have shown for the first time that αB-crystallin is present in both luteal and interstitial cells of corpus luteum. Furthermore, we showed translocalization of αB-crystallin in luteal and interstitial cells during CL life span and its correlation with the tubulin cytoskeletal system.

These results shed light on the role of αB-crystallin as chaperone, one possible role of which is to stabilize the cytoskeleton in different CL cell types during the CL formation and active functioning. Events that cause luteolysis induce relocalization of αB-crystallin in luteal and interstitial cells that may decrease chaperone activity of αB-crystallin and, in spite of the total amount of the protein in CL tissue, will cause apoptosis.

Acknowledgements

This work was supported in part by Estonian Science Foundation grants No. 1406 and 4524.

Alfa B-kristalinas tariamai vaikingų žiurkių geltonajame kūne

Raivo Masso, Anu Saag, Andres Arend[1], Marika Masso, Gunnar Selstam[2]

Tartu universiteto Bendrosios ir molekulinės patologijos katedra, [1]Anatomijos katedra, Estija, [2]Umeå universiteto Ląstelių ir molekulinės biologijos katedra, Švedija

Raktažodžiai: mažo terminio šoko baltymas, alfa B-kristalinas, geltonasis kūnas, imunohistochemija, ląstelės griaučiai.

Santrauka. Siekiant nustatyti αB-kristalino buvimo vietą ir lygį tariamai vaikingų žiurkių geltonajame kūne, naudotas šviesinis ir elektroninis imunohistocheminis mikroskopavimas. Antrą ir aštuonioliktą tyrimo dieną αB-kristalino buvo rasta žymiai didesnis kiekis palyginus su tuo, kuris buvo matomas geltonojo kūno žydėjimo stadijos metu (šešta ir dešimta diena). Alfa B-kristalino rasta geltonojo kūno luteininėse bei intersticinėse ląstelėse.

Atlikus šviesinę mikroskopiją, nustatyta, kad per geltonojo kūno egzistavimo laikotarpį alfa B-kristalino kiekis luteininių ląstelių citoplazmos centrinėje dalyje sumažėjo, o aplink plazmolemą – padidėjo. Intersticinėse ląstelėse alfa B-kristalino kiekis labiausiai padidėjo šeštą dieną, o funkcinės luteolizės metu alfa B-kristalinas beveik išnyko (penkiolikta ir aštuoniolikta diena).

Elektroninio mikroskopavimo metu gauti duomenys rodo, kad alfa B-kristalino esama citoplazmoje, taip pat netoli endoplazminio tinklelio, Goldžio komplekso, mitochondrijų, taip pat ir luteininių bei ląstelių branduoliuose. Antrą dieną alfa B-kristalino buvo gausu luteininių ląstelių citoplazmoje, bet mažai branduolyje. Geltonojo kūno žydėjimo ir funkcinės luteolizės laikotarpiu alfa B-kristalinas luteininėse ląstelėse pakeitė savo vietą ir buvo matomas aplink plazmolemą ir branduolį. Luteininių ląstelių branduoliuose alfa B-kristalino buvo labai nedaug. Tuo pat metu (šeštą dieną) intersticinėse ląstelėse, įskaitant ir jų branduolius, buvo daug alfa B-kristalino, kurio kiekis luteluteolizės metu buvo žymiai sumažėjęs.

Imunohistochemiškai aptinkamo tubulino sumažėjo geltonojo kūno audinyje per geltonojo kūno egzistavimo laikotarpį. Taigi galima manyti, kad alfa B-kristalinas veikia kaip palydovas, kurio viena iš galimų funkcijų – stabilizuoti ląstelių griaučius įvairių geltonojo kūno ląstelių tipuose geltonojo kūno formavimosi ir aktyvaus funkcionavimo laikotarpiais.

Adresas susirašinėjimui: R. Masso, Department of General and Molecular Pathology, University of Tartu, Ravila 19, 50411 Tartu, Estonia. El. paštas: masso@ut.ee

References

1. Clark JI, Muchowski PJ. Small heat-shock proteins and their potential role in human disease. Curr Opinion Structural Biol 2000;10:52-9.
2. Narberhaus F. α-Crystallin-type heat shock proteins: socializing minichaperones in the context of a multichaperone network. Microbiol Mol Biol Reviews 2002;66:64-93.
3. Nicholl ID, Quinlan RA. Chaperone activity of alpha-crystallins modulates intermediate filament assembly. EMBO Journal 1994;13:945-53.
4. Lowe J, McDermott H, Pike I, Spendlove I, Landon M, Mayer RJ. αB-crystallin expression in non-lenticular tissues and selective presence in ubiquitinated inclusion bodies in human disease. J Pathol 1992;166:61-8.
5. Kato K, Ito H, Inaguma Y, Okamoto K, Saga S. Synthesis and accumulation of alpha B-crystallin in C6 glioma cells is induced by agents that promote disassembly of microtubules. J Biol Chem 1996;27:26989-94.
6. Lehr HA, Mankoff DA, Corwin D, Santeusanio G, Gown AM. Application of photoshop-based image analysis to

quantification of hormone receptor expression in breast cancer. J Histochem Cytochem 1997;45:1559-65.
7. Voorter CE, Wintjes L, Bloemendal H, de Jong WW. Relocalization of alpha B-crystallin by heat shock in ovarian carcinoma cells. FEBS Lett 1992;309:111-4.
8. Klemenz R, Fröhli E, Steiger RH, Schäfer R, Aoyama A. αB-crystallin is a small heat shock protein. Proc Natl Acad Sci USA 1991;88:3652-56.
9. Salvador-Silva M, Ricard CS, Agapova OA, Yang P, Hernandez MR. Expression of small heat shock proteins and intermediate filaments in the human optic nerve head astrocytes exposed to elevated hydrostatic pressure in vitro. J Neurosci Res 2001;66:59-73.
10. Bennardini F, Wrzosek A, Chiesi M. αB-crystallin in cardiac tissue. Association with actin and desmin filaments. Circ Res 1992;71:288-94.
11. Arai H, Atomi Y. Chaperone activity of αB-crystallin suppresses tubulin aggregation through complex formation. Cell Struct Funct 1997;22:539-44.
12. Djabali K, De Nechaud B, Landon F, Portier MM. αB-crystallin interacts with intermediate filaments in response to stress. J Cell Sci 1997;110:2759-69.
13. Khan-Dawood FS, Yusoff Dawood M, Tabibzadeh S. Immunohistochemical analysis of the microanatomy of primate ovary. Biol Reprod 1996;54:734-42.
14. Murdoch WJ. Microtubular dynamics in granulosa cells of periovulatory follicles and granulosa-derived (large) lutein cells of sheep: relationships to the steroidogenic folliculo-luteal shift and functional luteolysis. Biol Reprod 1996;54: 1135-40.
15. Selstam G, Nilsson I, Mattsson MO. Changes in the ovarian intermediate filament desmin during the luteal phase of the adult pseudopregnant rat. Acta Physiol Scand 1993;147:123-9.
16. Nilsson I, Mattsson MO, Selstam G. Presence of the intermediate filaments cytokeratins and vimentin in the rat corpus luteum during luteal life-span. Histochem Cell. Biol 1995;103:3237-42.
17. Wang K, Spector A. Alpha-crystallin stabilizes act in filaments and prevents cytochalasin-induced depolymerization in a phosphorylation-dependent manner. Eur J Biochem 1996; 242:56-66.
18. Perng MD, Cairns L, van den Ijssel P, Prescott A, Hutcheson AM, Roy A et al. Intermediate filament interactions can be altered by HSP27 and αB-crystallin. J Cell Science 1999;112: 2099-112.
19. Bhat SP, Hale IL, Matsumoto B, Elghanayan D. Ectopic expression of alpha B-crystallin in Chinese hamster ovary cells suggests a nuclear role for this protein. Eur J Cell Biol 1999;78:143-50.
20. Xiao WM, Yuan KY, Xiao XZ, You JL, Zhong L. Heat shock pretreatment increases alpha B-crystallin expression and protects cardiomyocytes against injury induced by hydrogen peroxide. Hunan Yi Ke Da Xue Xue Bao 2000;25:223-26.
21. Shchors K, Yehiely F, Kular RK, Kotlo KU, Brewer G, Deiss LP. Cell death inhibiting RNA (CDIR) derived from a 3'-untranslated region binds AUF1 and heat shock protein 27. J Biol Chem 2002;277:47061-72.
22. Lasa M, Mahtani KR, Finch A, Brewer G, Saklatvala J, Clark AR. Regulation of cyclooxygenase 2 mRNA stability by the mitogen-activated protein kinase p38 signaling cascade. Mol Cell Biol 2000;20:4265-74.
23. Kamradt MC, Chen F, Cryns VL. The small heat shock protein αB-crystallin negatively regulates cytochrome c- and caspase-8-dependent activation of caspase-3 by inhibiting its autoproteolytic maturation. J Biol Chem 2001;276:16059-63.
24. Kamradt MC, Chen F, Sam S, Cryns VL. The small heat shock protein αB-crystallin negatively regulates apoptosis during myogenic differentiation by inhibiting caspase-3 activation. J Biol Chem 2002;277: 38731-6.
25. Ito H, Okamoto K, Nakayama H, Isobe T, Kato K. Phosphorylation of alpha B-crystallin in response to various types of stress. J Biol Chem 1997;272:29934-41.
26. Ito H, Hasegawa K, Inaguma Y, Kozawa O, Kato K. Enhancement of stress-induced synthesis of HSP27 and αB-crystallin by modulators of the arachidonic acid cascade. J Cell Physiol 1996;166:332-9.
27. Sawyer HR, Niswender KD, Braden TD, Niswender GD. Nuclear changes in ovine luteal cells in response to PGF2α. Domest Anim Endocrinol 1990;7:229-38.
28. Kerr JF, Wyllie AH, Currie AR. Apoptosis: a basic biological phenomenon with wide-ranging implications in tissue kinetics. Br J Cancer 1972;26:239-57.

Received 13 June 2003, accepted 23 September 2003
Straipsnis gautas 2003 06 13, priimtas 2003 09 23